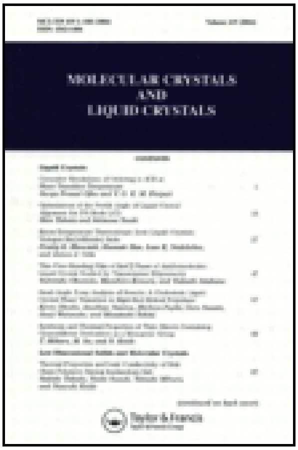

Molecular Crystals and Liquid Crystals Science and Technology. Section A. Molecular Crystals and Liquid Crystals

Publication details, including instructions for authors and subscription information:
http://www.tandfonline.com/loi/gmcl19

Aspects of Intercalation of Fluorine and Metal Fluorides into Graphite

Alain Tressaud [a]

[a] Laboratoire de Chimie du Solide du CNRS, Université de Bordeaux I, 33405, Talence Cedex, France

Version of record first published: 23 Oct 2006.

To cite this article: Alain Tressaud (1994): Aspects of Intercalation of Fluorine and Metal Fluorides into Graphite, Molecular Crystals and Liquid Crystals Science and Technology. Section A. Molecular Crystals and Liquid Crystals, 244:1, 13-28

To link to this article: http://dx.doi.org/10.1080/10587259408050077

Mol. Cryst. Liq. Cryst. 1994, Vol. 244, pp. 13–28
Reprints available directly from the publisher
Photocopying permitted by license only

Printed in the United States of America

ASPECTS OF INTERCALATION OF FLUORINE AND METAL FLUORIDES INTO GRAPHITE

Alain TRESSAUD
Laboratoire de Chimie du Solide du CNRS, Université de Bordeaux I,
33405 TALENCE Cedex, France

ABSTRACT - The peculiar reactivity of fluorine with graphite can be related to some characteristic parameters of this element. The competition between strong C-F bonds in covalent graphite fluorides and weak semi-ionic bonds in graphite intercalation compounds is pointed out. The different experimental routes for the intercalation of fluorine and metal fluorides into graphite are reviewed. The oxidation state, the environment of the metal and the nature of the bonding between the intercalated species and carbon can be approached by various techniques, including XANES, EXAFS, and XPS spectroscopies. The structural relationships between the graphene sublattice and the intercalate sublattice can be pointed out on the basis of single crystal data. Concerning the transport properties, acceptor-GICs have proved to be very appropriate to investigate the effects of disorder and reduced dimensionality. The charge transfer which accompanies the insertion of fluorinated species between the graphene layers can be evaluated from optical reflectivity and the subsequently calculated conductivity is compared with direct electrical data. In fibrous samples, disorder-induced phenomena are evidenced in both electrical and thermal transport properties. The electrical resistivity results can be analyzed in the framework of weak localization and carrier-carrier interaction models for 2D disordered electron systems.

ON THE REACTIVITY OF FLUORINE AND FLUORIDES ON GRAPHITE

Fluorine has been called the cornerstone of Mendeleev's periodic table. The peculiar properties of this element arise from a very high electronegativity : the redox potential of the F_2/F^- system is 2.87 V, with respect to a standard hydrogen reference. This high electronegativity gives rise to a small polarizability of the fluoride ion. The van der Waals radius is smaller than those of oxygen and chlorine (Table I). In addition in the halogen gas series, gaseous F_2 has a smaller dissociation energy than Cl_2 and Br_2.

The subsequent high reactivity of fluorine results in the formation of a very wide range of fluorides with most elements [1]. However, when compared with corresponding inorganic oxides for instance, fluorides are generally less stable

TABLE I - Relevant parameters of oxygen, fluorine and chlorine

	O	F	Cl
Electronegativity (Allred and Rochow scale)	3.5	4.1	2.8
Polarizability ($x10^{24}$ cm^3)	3	0.81	2.98
Van der Waals radius (Å)	1.40	1.35	1.86
Dissociation energy (kcal.mol^{-1})	118	36	57

thermodynamically, because M-F bonds are weaker than M-O bonds. In the latter ones indeed, π bonding is enhanced by the high charge of O^{2-}, resulting in slightly smaller M-O distances.

Only fluorine and oxygen react with carbon to form covalent bonds giving so-called graphite fluoride and graphite oxide. In the case of chlorine, the larger van der Waals radius, the lower electronegativity, and higher dissociation energy than those of fluorine hinder the formation of "graphite chloride" and only a surface adsorption of Cl_2 is observed.

Evidence of the exceptional properties of fluorine, i.e. :

- extremely high electronegativity,
- weak polarizability,
- small size of fluorine atom,
- high reactiviy due to low dissociation energy,

is clearly given by the reactivity of this element with carbon atoms forming the graphite structure. The main point is the **competition between the strong C-F bond in covalent graphite fluorides and the weak semi-ionic C-F bond in graphite intercalation compounds (GICs).**

Depending on experimental conditions indeed, the fluorination of graphite may give rise to the formation of strong C-F bonds with a corresponding sp^3 hybridization of electronic orbitals of carbon, in the case of so-called graphite fluorides $(CF)_n$ and $(C_2F)_n$, when the thermal energy brought to the system is large enough (T_{F_2} > 350°C) ; on the other hand the fluorination may also lead to intercalation compounds with semi-ionic C-F bonds. These latter compounds are obtained by low-temperature reactions (T_{F_2} < 100°C) in the presence of additives or catalytic species (HF, metal fluorides and chlorides, ...).

It has been assumed that the absence of reaction between pure F_2 and graphite at low temperature could be a kinetic problem connected with the small size of fluorine [2]. Since fluorine cannot form larger species (such as F_3^-) the only possible reaction, i.e. that giving rise to covalent C-F bond with C atoms, does not provide any step for a further migration of fluorine in the interplane layer and prevents the reaction to proceed. The presence of HF or of traces of metal fluorides during the fluorination process would allow the formation of larger $[(HF)_nF]^-$ or $(MF_n)^-$ species which have a lower trend to react with C atoms of the graphene layers, reducing therefore the kinetic barrier and considerably increasing the intercalation rate.

In the charge transfer that occurs during the intercalation of graphite by fluorine or by fluorides, the intercalates are expected to be electron acceptors. Among the numerous methods that have been used to establish the nature of the carriers and to evaluate the magnitude of the charge transfer, we give below as examples three very different experimental approaches.

* **Decrease of the C-C bond length** - In electron acceptor GICs, a contraction of C-C bond length is observed because of the contribution of π antibonding orbitals. An empirical relationship has been proposed by S.Flandrois et al. between charge transfer and C-C bond length [3]. This empirical relationship obtained from experimental data of several acceptor GICs, including Ru pentafluoride, is compared in Fig. 1 with theoretical calculations from Pietronero and Strässler (P.S.) and Chan et al. (CKHE).

* **Determination of the nature on the intercalated species by X-ray absorption spectra** -The position of the absorption edge and the shape of the absorption spectra give information on the oxidation state and on the environment of the concerned element. N. Bartlett has shown, using X-ray absorption at As K edge, that the intercalation of AsF_5 in graphite (HOPG) could proceed according to the reaction [4]:

$$3AsF_5 + 2e \rightarrow AsF_3 + 2AsF_6^- .$$

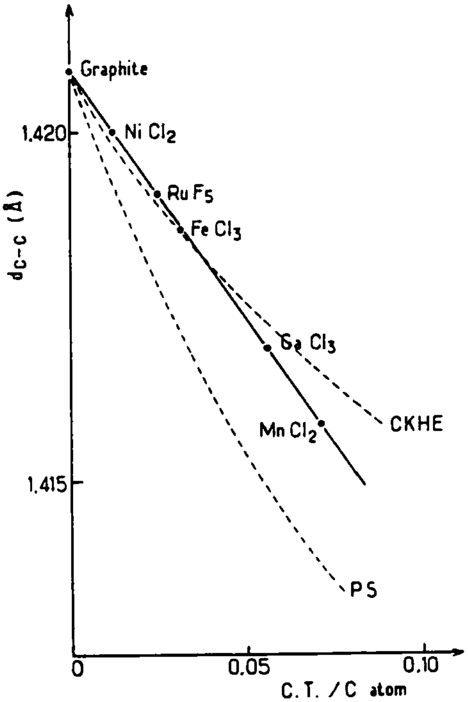

FIGURE. 1 - Decrease of C-C bond length in some acceptor GICs as a function of charge transfer [3].

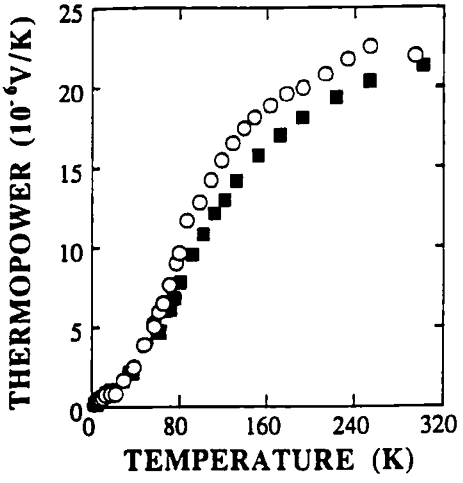

FIGURE 2 - Temperature dependence of the thermoelectric power of HOPG-based metal fluoride-GICs [chromium fluoride based (■), gold fluoride-based (o)].

These results were also confirmed in the case of PAN-based fibers [5]. The electrons are trapped from the graphene layers and the drastic increase of electrical conductivity which results is due to the increase of charge carrier density by injection of holes into the graphite layer from the intercalate.

* **Thermoelectric power** - The measurement of the thermoelectric power (TEP) allows the determination of the sign of the carrier type dominating the transport properties. For instance, Fig. 2 shows the temperature dependence of the in-plane TEP for several metal fluoride-based GICs [6]. The curves follow the general trend observed for acceptor GICs, whatever the stage and the involved intercalate. After increasing from low temperature, the TEP reaches a broad maximum around 200-300 K with corresponding positive values of $\approx$ 20 μV K^{-1} that is the signature of hole carriers.In the F-intercalated GIC C_4F the value of the maximum TEP ($\alpha = 16\mu VK^{-1}$) is slightly lower than those of other stage-2 acceptor GICs [7].

The interest of the subject can be accounted for by the publication of several books that appeared recently dealing with the reactivity of fluorine with graphite and giving informations on the different types of materials-covalent graphite fluorides or GICs - that can be obtained ["Inorganic Solid Fluorides", P. Hagenmuller ed. Academic Press (1985); "Graphite Fluorides" N. Watanabe, T. Nakajima and H. Touhara, Elsevier (1988) "Graphite Fluorides and Carbon-Fluorine Compounds", T. Nakajima and N. Watanabe, CRC Press (1991)].

In the next sections we first summarize the different experimental routes that have been proposed to intercalate fluorine and fluorides in graphite. We select after some examples on the structural characterization of these materials mainly for transition metal fluorides GICs and finally we give some insight on recent results on transport properties of F- and metal fluoride - GIC's.

It can be noted that in the following the fluorine-GICs are often abbreviated as C_xF, instead of more complete formulations $C_xF_{1-\delta}(HF)_\delta$ or $C_xF_{1-\delta}(MF_n)_\delta$, δ being very small.

EXPERIMENTAL ROUTES FOR THE INTERCALATION OF FLUORINE AND METAL FLUORIDES INTO GRAPHITE

Concerning the preparative methods (for instance synthesis of the starting fluorides, handling procedures, nature of materials and equipments that can be used in the presence of fluorinating gases and reagents, ...) several review papers recently appeared, dealing with the technical requirements : see for instance J. Grannec and L. Lozano (1985) [8], [9], [10], and references herein.

The starting metal fluorides are often obtained via gas-solid reactions using either F_2 gas or HF gas. However, depending on the required materials, other methods can be used, which include reactions in solution, in non-aqueous solvents, solid state reactions, decomposition processes [8]. The materials that can be used in the "fluorination lines" are either fluoropolymers or metals. A combination of both types often provide a convenient reaction system [11]. Concerning the intercalation procedure, two main routes can be considered depending whether the reaction occurs in the gas state or in the liquid state.

Intercalation in the gas state

* **Fluorine** - As previously noted, when highly purified F_2 gas is used, no noticeable reaction occurs with graphite up to 300°C. Since the early works of W. and G. Rüdorff, gaseous HF has been largely used to promote the intercalation of fluorine [12-14].

The reaction takes place at room temperature in a mixture of fluorine gas and gaseous HF (less than 30%). In the first stage of the reaction, the highly mobile $(HF_2)^-$ species are rapidely intercalated to give stage-3 or stage-2 C_xHF_2 (the higher content of $(HF_2)^-$ corresponds to the $C_{11}HF_2$ composition), then the fluorine species progressively substitute the HF_2^- groups. After a period of about 2 days stage-1 compounds are obtained, with the general formula ; $C_xF_{1-\delta}(HF)_\delta$, with $2<x<5\text{-}6$ and $\delta \approx x/12$ [14]. In this large range of compositions the unit cell parameters varie continuously and also the resistivity which is generally higher than that of pristine graphite [14]. Even for high fluorine contents the products are black and insensitive to moisture. When vacuum-treated they lose some HF from 150°C [14].

Many different additives have been used to assist the F_2 intercalation process ; they are generally high Lewis acids :

- involatile fluorides (AgF, CuF_2, LiF) $\longrightarrow$ stage 1 to 4 - C_4F to $C_{16}F$ [15] ,
- volatile pentafluorides (AsF_5, IF_5) $\longrightarrow$ stage 1 to 4 - C_2F to $C_{16}F$ [16-19],
- volatile fluorides (WF_6, MoF_6, IF_5,...) $\longrightarrow$ stage 1 - $C_{1.33}F$ to C_4F [20] .

In several cases an intermediate GIC is formed with the corresponding fluoride, as proposed by A. Hamwi et al. and is further replaced by the C_xF phase [20], as in the case of HF additive. It can be noted that "unclean" conditions may also be favorable, since F_2 will react on adsorbed H_2O molecules to give rise to traces of HF. The arrangement of the intercalates in the galleries is not clear, in particular for important fluorine concentrations, and the influence of the nature of the added fluoride has not yet totally been solved . Several hypotheses have been proposed to explain the peculiar features of stage-1 materials [21-23].

* **Main group and transition metal fluorides** - Concerning the intercalation of main group - and transition metal fluorides, most of hexafluorides and pentafluorides have been inserted using this way and a complete review on the chemistry [24-27] and physics [28-30] of GICs is available.

Let us note that some fluorides intercalate spontaneously (i.e. AsF_5, SbF_5, RuF_5, OsF_5, OsF_6) whereas others require the use of an oxidative medium, such as fluorine (i.e. IF_5, PF_5, BF_3, GeF_4, TiF_4, WF_6, ...). The reaction is generally carried out at low temperature (below 250°C) in order to avoid the deintercalation process and a wide range of different stages have been obtained.

Intercalation in the liquid - or molten - state

The intercalation of fluorine in graphite can also be realized in liquid HF after a careful purification of the medium to avoid even traces of moisture. Fluorine is added either by bubbling F_2 gas in the liquid [31] or by decomposing prior to the reaction inorganic fluorides containing a transition element at a higher oxidation state[38, 39].

An electrochemical fluorination of graphite in liquid HF leads to stage-1 or stage-2 $C_xF_{1-\delta}(HF)_\delta$; with progress of the reaction the number of HF groups tends to decrease and to be substituted by fluorine, as in the case of F_2-gas method. When the fluorine rate increases (x decreasing from 5 to 2), the width of the intergraphene gallery increases from 5 Å to more than 6 Å [32, 33]. The stability of the intercalate after evacuation and the change in C-F bonding have also been investigated : stage-1 GICs with semi-ionic bonds keep their structure even when vacuum treated.

In the dissociation equilibrium $KF.2HF \Leftrightarrow K^+ + HF_2^- + HF$ which is present in molten KF.2HF at around 100°C, the vapour pressure of HF is much lower than in liquid HF. The electrochemical intercalation of fluorine is observed only for highly dehydrated melt and gives rise to stage-4 C_xHF_2. When LiF is added to the melt, the intercalation is improved, yielding a stage-3 material [34].

A new method to prepare C_xF via metal fluoride-GICs has been recently proposed: when stage-2 or stage-3 $CxAsF_6$ are treated with fluorine in liquid HF at room temperature, a C_xF phase with very high fluorine content ($x_{min} \approx 1.3$) is formed with stage-1 $CxAsF_6$ [35]. The C_xF phase is then isolated by destructive oxidation of the C_xAsF_6 compound with perchloric acid.

Investigations are still needed to have a better understanding of similarities and differences of $CxF_{1-\delta}(HF)_\delta$ phases obtained from these various conditions.

Using the same anhydrous HF medium, the intercalation of metal fluorides can be achieved at room temperature when the solubility in HF of the involved fluoride is high enough. Fluorine may be added, as reported above, by bubbling F_2-gas in the liquid HF. By this method stage-2 GICs obtained from SnF_4 and PbF_4 have been prepared (possibly through an intermediate C_xHF_2 compound) [36]. The fluorine may also be provided by decomposing inorganic fluorides in the liquid HF prior to reaction. In the involved fluorides the cation is present in a high oxidation state, such as Mn(+III), Ni(+IV), Cu(+III) [37]. This method has been thorouglhy used in the case of the intercalation of d-transition metal fluorides : $CrF_4 + CrF_5$, RhF_3, AuF_3 [38,39]

It can be now pointed out the great importance of the starting host material. Graphite is available in very different forms. The types most investigated are : powder (for instance SP1) ; natural flaky samples (NG) from Madagascar or Ceylon ; highly oriented pyrolytic form (HOPG) ; three main types of fibers i) ex-polymer (PAN derived), ii) ex-pitch (PDF), iii) vapor-grown (VGCF). It is clear that the type of starting material will be choosen with respect to the property to be investigated. The determination of most of structural and physical properties require the use of best crystallized materials i.e. NG or HOPG. However, due to their important applied interest, the intercalation process in graphite fibers has been largely developed (see for instance chapter 8 in "Graphite Intercalation Compounds" II by M.S. Dresselhaus and M. Endo [30]. The fluorine intercalation procedure in fibers is carried out in F_2 atmosphere with the help of different types of additives : metal fluorides CuF_2, AgF [40-42], or HF [43]. It has been claimed that the intercalation of AsF_5 in vapor-grown fibers yields very high electrical conductivity ($\sigma_{300\ K} \approx 9 \times 10^5$ S cm^{-1}) [44], but this result needs further confirmation.

STRUCTURAL CHARACTERIZATION OF METAL FLUORIDE-GICs

Determination of the oxidation state of the transition element

Since a wide range of oxidation states is available in transition-metal fluorides, the determination of the final electronic configuration of these elements after intercalation is of decisive interest.

The number of unpaired d-electrons directly affects the magnetic properties which have been therefore one of the methods most largely used. In the intercalation process of d-metal hexafluorides, it has been shown that (+V) oxidation state was obtained in the case of C_8OsF_6 and C_8IrF_6, whereas in the case of PtF_6, the intercalation yielded a higher oxidation of graphite, giving rise to a Pt(IV) compound: $C_{12}PtF_6$ [4].

On the other hand, the diamagnetic properties of TiF_4-GICs or RhF_3-GICs clearly indicate the presence of Ti(+IV) and Rh(+III) in these compounds [38,45].

In the case of the intercalation of Ru pentafluoride the magnetic properties of stage-1 $C_{5.2}RuF_{4.5}$ completely differ from those of pure pentafluoride [3] . However similar paramagnetic θp confirm the presence of strong antiferromagnetic interactions between Ru atoms. The effective moment of the GIC ($M_{eff} = 3.14 \pm 0.09 \mu_B$) is close to that calculated for Ru(+IV) [$M_{eff} = 2.9\ \mu_B$ for $S = 1$ and $g = 2$], whereas that expected for Ru(+V) is $M_{eff} = 3.9 \mu_B$ for $S = 3/2$ and $g = 2$] [3]. The presence of segments of chains of (RuF6) octahedra sharing edges has been proposed in relation with the single crystal data. The presence in $C_{5.2}RuF_{4.5}$ of 25% of $(RuF_6)^{2-}$ isolated octahedra together with 75% of $(RuF_4)_n$ chains would be a possible solution to achieve the $RuF_{4.5}$ stoichiometry and to take into account analytical, magnetic and crystallographic data.

More recently X-ray absorption spectroscopy has proved to be a powerful tool to elucidate structural problems in ill-crystallized materials. In the part of the spectrum which is situated at energies close to the absorption threshold, i.e. in the XANES domain, the position and the envelope of the spectrum depend on different physical parameters, including site symmetry, formal and effective charge of the absorbing atom [46]. In the case of the intercalation of CrF_4 in graphite, the presence in the XANES domain of a peak in the pre-threshold region at the same energy ($E = 5994$ eV) for $Na_2Cr^{IV}F_6$ and $C_{21}CrF_{4.5}$ indicates that the oxidation state of intercalated chromium is (+IV) [47]. The observed peak, which corresponds to an 1s → 3d quadrupolar transition is enhanced for increasing oxidation states because of the higher number of empty d orbitals [46].

In the case of tin fluoride -GICs, a ^{119}Sn Mössbauer resonance investigation has been performed on HOPG-based $C_{30}SnF_5$. The value of the isomer shift clearly indicates that Sn is present in the (+IV) oxidation state [48]. From the value of the isomer shift and from EXAFS data, it has been assumed that the distortion of the shell of first nearest neighbors of Sn(IV) is similar to that of SnF_4, whereas the long range totally differs, giving rise to different quadrupole splitting values. The assumption of corner-shared SnF_6 octahedra with faces parallel to the graphite layer has been raised. These groups would be condensed in clusters of average composition SnF_5 with variable extension.

Evaluation of charge transfer in d-transition metal fluoride-GICs

We have seen in section I that the accurate determination of the variation of C-C bond length in the graphene layer after intercalation could be correlated to the charge transfer rate [49] (see Fig. 1). In the case of ruthenium fluoride-GIC, the determination of the position of (110) reflection in a single crystal (NG) of $C_{20}RuF_{4.5}$ composition confirms the contraction bond length $d_{C\text{-}C}$ = 1.4191(4) Å compared to that of pristine graphite $d_{C\text{-}C}$ = 1.4209(1) Å. From the relationship given in Fig. 1, it corresponds to a charge transfer of 0.025 e per C atom, i.e. 0.5 e per intercalated $RuF_{4.5}$ group.

The charge transfer coefficient (f) can also be determined from optical reflectivity. In most of d-transition metal fluoride-GICs, a metallic reflectivity is observed in the low-frequency region of the spectra, limited by the plasma edge and followed by a well-defined minimun [50]. The position of the Fermi energy (E_F) can be deduced through the Blinowski-Rigaux model [51]. In Table II are reported E_F and charge transfers for several GICs. The electrical conductivity deduced from optical reflectivity data (σ_{opt}) is compared with the experimental data measured by the contactless method (σ_{clm}). It can be noted some discrepancies for paramagnetic Cr(+IV) or Ir(+IV) fluoride-GICs whereas relatively close values are obtained for diamagnetic $C_xAu^{III}F_{3.2}$.

Table II - Parameters obtained from the fitting of the experimental data using the Blinowski-Rigaux model [* the compositions have been deduced from elemental analysis)].

Compounds* (HOPG-based)	Stage	I_c(Å)	E_F(eV)	τ(s) 10^{-14}	f_C	f_m	σ_{opt} (S cm^{-1})10^4	σ_{clm} (S cm^{-1})10^4
$C_{21}CrF_{4.5}$	2	11.45	0.94	2.8	0.024	0.50	5.2	0.7
$C_{28}RhF_{3.3}(HF_2)_{1.3}$	2	11.25	0.89	1.2	0.021	0.59	2.2	-
$C_{14.4}IrF_{4.8}$	2	11.47	1.03	0.73	0.023	0.33	1.5	0.65
$C_{12.5}AuF_{3.2}$	2	11.57	0.97	1.06	0.020	0.25	2.0	1.94

It can be pointed out that in most of these GICs the evaluated charge transfers correspond to close values and can be compared to that proposed for AsF_5-GIC which ranges from 0.2 to 0.5 e per intercalate [4].

Determination of the environment of the inserted cation by EXAFS

The EXAFS modulation at the metal edge are analyzed following conventional procedures [52-54]. One important point is the use of standards exhibiting composition and characteristics as close as possible to those expected for the intercalate. These reference compounds provide the experiments with backscattering amplitude and with phase shifts. If such standards are not available, Teo and Lee functions may be used.

The same Hanning window has to be chosen for both standard and GIC samples to perform the Fourier transforms of the k^3 - weighted EXAFS signals. The obtained radial structure functions at a distance R(Å) of the metal absorber atom, uncorrected from phase shift are given in Fig. 3-a for GICs based on Rh fluoride or on Au fluoride for instance. A damping of the signal occurs for the GICs after the first coordination shell because of the disordering of the intercalates. This effect unfortunately restricts the investigations in this type of materials to the first neighbors. The first peak between 1.2 Å and 1.9 Å corresponds to the first neighbor coordination shell. The peaks are back-transformed to lead to filtered EXAFS functions. In the case of the Rh compound, the backscattered phases and retrodiffusion amplitudes are extracted from a standard sample (RhF_3), whereas in the case of the Au compound, Teo and Lee functions are used, in the absence of any gold fluoride stable in air. The good agreement of the least square fitting of the Fourier-filtered spectra are shown in Fig. 3b. The resulting number of fluorine atoms (N) constituting the first coordination sphere at a distance R from the metal absorbers are given in Table III.

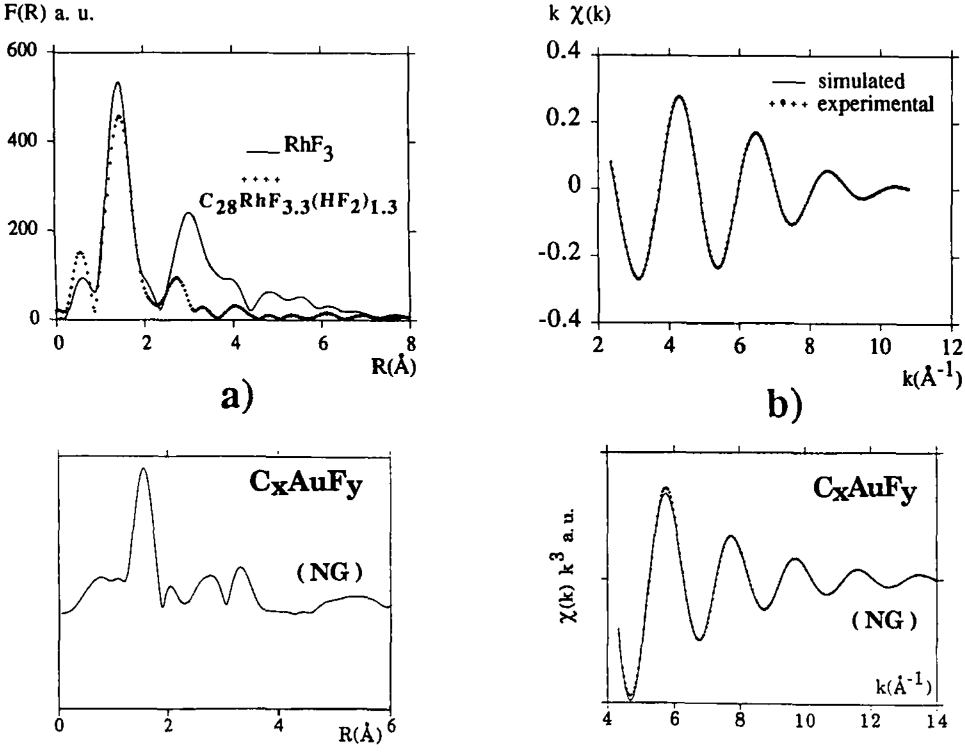

FIGURE 3- Determination of the environment of Rh and Au in metal fluoride-GICs : a) Radial structure functions, uncorrected for phase shift ; b) Fourier-filtered EXAFS functions [experimental values (+) are compared with curves obtained by least square fitting (solid lines)].

TABLE III - Structural informations deduced from EXAFS results

	N	R(Å)	σ^2(Å^2)
(HOPG-based) C_xRhF_y	6.0±0.3	1.99±0.02	0.0036
(NG-based) C_xAuF_y	2.9±0.3	2.08±0.02	0.0049
	1.0±0.1	2.00±0.02	0.0009

In the case of Rh-based materials, the similarity of the peaks corresponding to the first neighbors in both RhF_3 and GIC (modulus of the Fourier transforms of Fig. 3a, together with the excellent fitting of the Fourier-filtered EXAFS spectra confirm the octahedral environment of the intercalated rhodium.

Concerning the Au-based GIC, the R and N values are in agreement with a square planar coordination that is generally associated with Au(+III) in its low-spin d^8 configuration. In the radial structure function a weaker second neighbor shell can be noted between 2.3 and 3 Å (Fig. 3a). Due to the rather large distance from the absorber, this signal should be assigned to an Au contribution ; a preliminary fitting gives a average distance Au-Au ≈ 2.9 Å. The structural data, as deduced from the EXAFS results, could correspond therefore to Au_2F_6 dimeric groups with approximately 2.9 and 5.9 Å edges. These dimers would be formed of two AuF_4 squares sharing a common edge. Their dimensions fit the hexagonal lattice of the intercalate (6.16 Å, a-edge) found from single crystal precession patterns.

ELECTRICAL AND THERMAL PROPERTIES OF F_2- AND METAL FLUORIDE-GIC's

One of the most outstanding property of acceptor-GICs is the enhancement of the electrical conductivity upon intercalation. This trend can be correlated to the increase of the intercalate concentration. The corresponding increase in the density of charge carriers is caused by injections of holes into the graphene layers from the intercalates. Generally the effect associated with the decrease in carrier mobility is not strong enough to affect the resulting value and an improvement of more than one order of magnitude may be observed. We will see later the particular case of highly fluorinated C_xF.

This behavior can be noticed for all types of starting graphite (HOPG, natural graphite, powder, fibers). However, the fiber geometry seems to be more appropriate to reduce the exchange with atmosphere. Intercalated fibers are generally insensitive to moist air (at least for several days or weeks), even for highly inserted materials, i.e. for stage-1 $C_{2-4}F$. On contrary, for similar intercalation rates, GICs based on other host materials are often unstable under moist air and undergo exchange or decomposition reactions that may proceed to complete deintercalation.

Fluorine-GICs

The transport properties of fluorine -GICs C_xF have been largely investigated these last years [7,42].The main features that can be pointed out are the following :

Contrary to other GICs in which intercalation always leads to an increase of conductivity with respect to the pristine materials, in the case of C_xF a maximum of conductivity is obtained for an optimal intercalate (charge carrier) concentration [7,19]. The highest conductivity values are obtained for VGCF-based compounds [43]. In Fig. 4 are shown for instance the temperature dependence of the resistivity of stage-3 compound $C_{10}F$. The room-temperature conductivity is as high as 1.6×10^5 Scm^{-1} . The magnitude of the anomaly which occurs around 180 K in fluorine-treated fibers increases with increasing fluorine contents. This effect is in good agreement with that observed by L. Piraux et al. on VGCF-based C_xF with higher fluorine contents ($4.1 \leq x \leq 5.8$) [7]. Thermal-expansion studies have shown that such an anomaly could be associated with a possible phase transition.

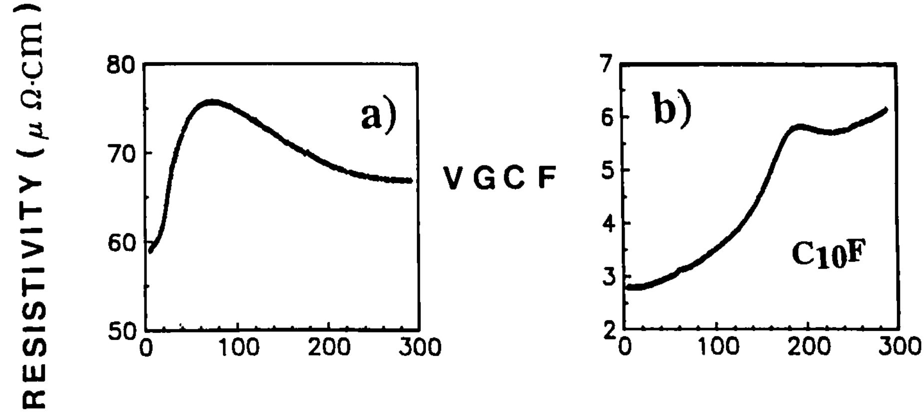

FIGURE 4 - Temperature dependence of the resistivity of a) pristine vapor grown fiber ; b) corresponding fluorine-treated fiber (stage-3 $C_{10}F$).

The very high anisotropy of the electrical conductivity of fluorine- and metal fluoride-GICs ($\sigma_a/\sigma_c \approx 10^6$ in C_xF [19]) allows to consider the charges-carrier system as a quasi -2D hole gas. Thanks to the large composition range available in these materials, 2D-disorder phenomena of electronic transport properties - such as weak localization effects - can be investigated by controlling the level of disorder. For $x \geq 4$, C_xF compounds are in the weak-disorder limit and exhibit a logarithmic variation of resistivity with temperature : the slope of the log T variation increases as x decreases. Similar trends in the low-temperature dependence of resistivity have been observed for both F-intercalated vapor-grown and pitch-derived fibers.

For VGCF-based stage-2 C_xF ($4 \leq x \leq 5.8$) each compound exhibits, when the temperature is lowered below 30 K, such logarithmic increase of resistivity. In this composition range, the magnitude of the effect is very sensitive to the fluorine content [7].

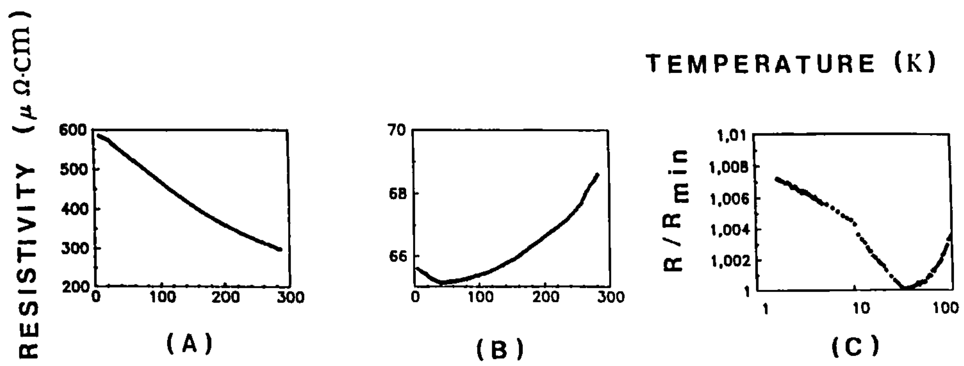

FIGURE. 5 - Temperature dependence of the resistivity of a) pristine pitch-derived fiber; b) corresponding fluorine-treated fiber (stage-3 $C_{11}F$) ; c) R/R_{min} variation [a) and b) linear temperature scale ; c) logarithmic temperature scale].

For stage-3 pitch-based C_xF ($11 \leq x \leq 13.5$) similar minimum is observed in the $\rho = f(T)$ curve (Fig. 5) [43].

In order to evaluate the relative contribution of weak localization and of Coulomb-type interactions, the infuence of a magnetic field on the temperature dependence of the resistivity has been investigated. It is known indeed, that the weak localization effect tends to vanish when a magnetic field is applied perpendicular to the 2D charge-carrier system, whereas the Coulomb-type interactions are no affected.

The large negative magnetoresistance effect which has been observed in VGCF-derived C_4F cannot be explained by the presence of unintercalated regions as it has been previously proposed ; pristine vapor-grown fibers actually exhibited a positive magnetoresistance. From these magnetoresistance experiments, the low-temperature dependence of resistivity has been interpreted by L. Piraux et al. in term of 2D carrier-carrier effects and to a weaker amount to weak localization [7].

The temperature dependence of the thermoelectric power of VGCF-based C_4F sample is similar to those previously observed for low-stage acceptor GICs. The estimation of the Fermi energy (E_F = 0.9 eV) using relations for the diffusion TEP in the scope of the Blinowski-Rigaux model, suggests that the carrier density is similar to those obtained in other low-stage acceptor GICs [7]. Therefore the high resistivity observed in this sample would be rather due to a low hole mobility.

For highly fluorinated stage-1 C_xF, a further increase of the intercalate concentration leads for $x < 0.4$ to a drastic decrease of conductivity. This decrease can be larger than one order of magnitude. For instance stage-1 C_xF prepared with traces of SbF_5 exhibits conductivity even lower (2.3×10^3 S cm^{-1}) than pristine HOPG [23]. Within each stage the fluorine concentration may vary and this point is particularly important in the lower stages, in which covalent C-F bonds are found besides the semi-ionic ones which exist on the whole range of C_xF composition.

For stage 1 F-GICs the high resistivities which are observed are due to strong defect scattering because of a pronounced distortion of the graphene layers. This increased distortion can be associated with the presence of covalent C-F bonds.

Metal fluoride-GICs

Most of metal fluoride-GICs behave a conventional metallic-type dependence of the resistivity. The still high value of the resistivity which is often observed might be due to a limited intercalation process. The hysteresis in resistivity which occurs for $C_xRuF_{4.5}$ around 130 K could result from the incommensurate ⇔ commensurate phase transition observed by X-ray diffraction [3].

The temperature dependence of the resitivity for various metal fluoride-GICs recently obtained from different graphite host materials is given in Fig. 6 . A logarithmic decrease of resistivity with increasing temperatures is observed for all samples when starting from low temperatures [2]. It can be pointed out that the nature of both the host material and the intercalate are prevailing for the magnitude of the phenomenon. For pitch-derived fibers intercalated by chromium fluoride or by rhodium fluoride this effect occurs over the whole temperature range, i.e. $1.5\ K < T < 300\ K$ (Fig. 6 a). The decrease of resistance on one decade of temperature is about 10 to 20%, depending on the sample. On the other hand, for HOPG samples intercalated with various fluorides, the logarithmic decrease of resisivity is limited to the low-temperature range only ($T \leq 30K$). The corresponding slope of $\rho = f(\ln T)$ is only 0.1 to 1% (Fig. 6 b). These results constitute with those of Meschi et al. [55] the only experimental proof for a low-temperature divergence of resistivity in intercalated HOPG materials.

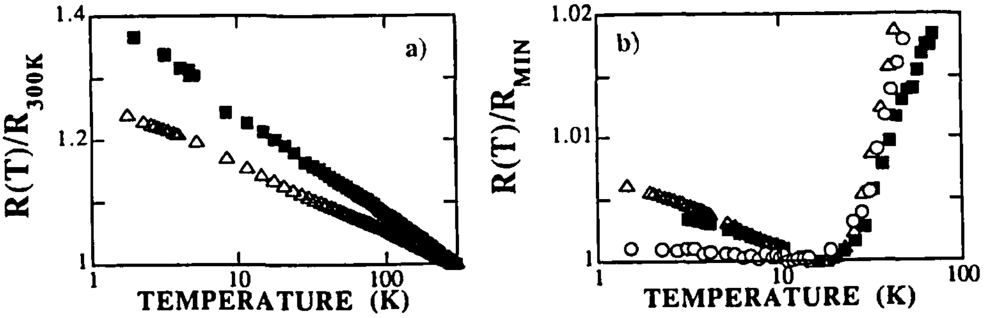

FIGURE 6 - Temperature dependence of the resistivity in a logarithmic temperature scale of various metal fluoride-GICs. a) pitch derived fibers stage-2 PDF-CrF_y (■) and stage-1 PDF-RhF_y (Δ) ; b) HOPG stage-2 C_xAuF_y (o), stage 2 C_xCrF_y (■), stage-2 C_xRhF_y (Δ). [The data are normalized to the room temperature value in a) and to minimum value in b)].

As in the case of C_xF compounds, the increase of resistivity observed down to low temperatures may be interpreted in terms of weak-localization and carrier-carrier interaction effects in the two-dimensional limit [6].

Concerning the effect of an external magnetic field on the temperature dependence of resistivity , a decrease in the slope is observed for H = 4T for instance in the case of VGCF-based chromium fluoride-GIC., which accounts for the disappearance of weak-localization effects under applied field [6] The remaining logarithmic dependence of resistivity is due to carrier-carrier contribution, as previously found for C_xF samples. The magnetoresistance effect is negative as shown in Fig. 7 for VGCF-based chromium fluoride GIC and increases with decreasing temperatures. These features are consistent with the weak-localization effect [7]. Both the H^2 variation predicted in the low-field limit and the ln H variation of the high-field limit are observed. The good agreement between experimental points and calculated curve [the solid lines of Fig. 7 correspond to the best fit] that is obtained over the whole range of magnetic fields demonstrates that the theorv of weak localization in the 2D limit convincingly accounts for the behavior observed for these compounds.

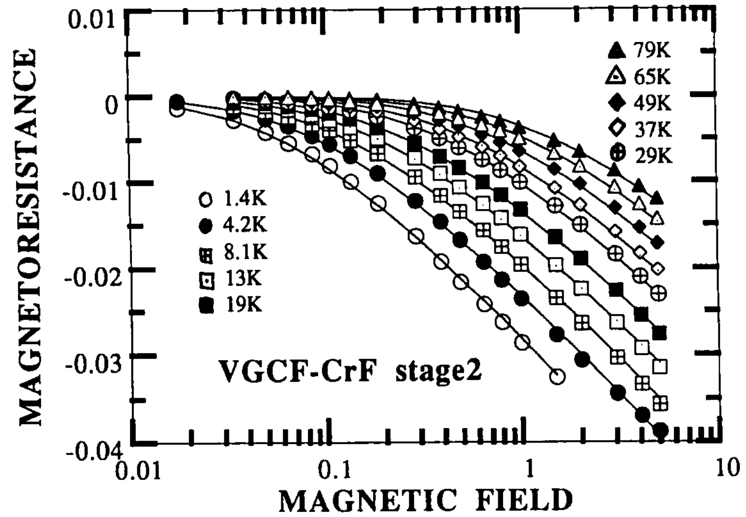

FIGURE 7 - Magnetoresistance vs. magnetic field for VGCF-based chromium fluoride-GIC. The solid lines are fits to the experimental data using weak-localization theory.

Acknowledgments - The author gratefully acknowledges Messrs. K. Amine, L. Fournès, J. Grannec, L. Lozano and S.M. Mayorga for constant help and interest and Messrs. S. Flandrois, J.P. Issi, T. Nakajima, L. Piraux and H. Touhara for fruitful collaboration and discussions.

REFERENCES

1 - D. Babel and A. Tressaud : Crystal Chemistry of Fluorides in "Inorganic Solid Fluorides", P. Hagenmuller ed., p. 77, Academic Press, New-York (1985).

2 - N. Bartlett in "Inorganic Solid Fluorides", P. Hagenmuller ed., p. 331, Academic Press, New York (1985).

3 - S. Flandrois, J. Grannec, C. Hauw, B. Hun, L. Lozano and A. Tressaud, J. Solid State Chem., **77**, 264 (1988).

4 - N. Bartlett, R.N. Bianconi, B.W. McQuillan, A.S. Robertson and A.C. Thompson, J. Chem. Soc. Chem. Commun., **200** (1978).

5 - S.M. Heald, H.A. Goldberg and I.L. Kalnin in "EXAFS and the Near Edge Structure", Springer Ser. Chem. Phys., **27**, 141, Springer, Berlin (1983).

6 - L. Piraux, K. Amine, V. Bayot, J.P. Issi, A. Tressaud and H. Fujimoto, Solid State Commun., **82**, 371 (1992).

7 - L. Piraux, V. Bayot, J.P.Issi, M.S. Dresselhaus, M. Endo and T. Nakajima, Phys. Rev. B **41**, 4961 (1990), Phys. Rev. B **45**, 14315 (1992).

8 - J. Grannec and L. Lozano : "Preparative Methods" in "Inorganic Solid Fluorides", P. Hagenmuller ed., p. 18, Academic Press, New-York (1985).

9 - N. Watanabe, T. Nakajima and H. Touhara, "Graphite Fluorides", Elsevier, Amsterdam (1988).

10 - T. Nakajima and N. Watanabe, "Graphite Fluorides and Carbon-Fluorine Compounds", CRC Press, Boca Raton (1991).

11 - N. Bartlett, Prep. Inorg. React., **2**,, 301 (1965).

12 - W. Rüdorff and G. Rüdorff, Z. anorg. allg. Chem., **253**, 281 (1947).

13 - R.J. Lagow, R.B. Badachhap, P. Ficalora, J.L. Wood and J.L. Margrave, Syn. Inorg. Metal-Org. Chem. **2**, 145 (1972).

14 - T. Mallouk and N. Bartlett, J. Chem. Soc. Chem. Commun., p. 103 (1983).

15 - T. Nakajima, M. Kawaguchi and N. Watanabe, Chem. Letters, p. 1045 (1981). Z. Naturforsch; **36b**, 1419 (1981) ; Carbon **20**, 287 (1982) ; Solid State Ionics **11**, 65 (1983) ; Synth. Metals 7, 117 (1983).

16 - I. Palchan, D. Davidov, and H. Selig, J. Chem. Soc. Chem. Commun, 657 (1983).

17 - D. Davidov, O. Milo, I. Palchan and H. Selig, Synth. Metals, **8**, 83 (1983).

18 - I. Palchan, D. Davidov , V. Zevin, G. Polatsek and H. Selig, Synth. Metals, **12**, 413 (1985).

19 - D. Vaknin, I. Palchan, D. Davidov, H. Selig and D. Moses, Synth. Metals, **16**, 349 (1986).

20 - A. Hamwi, M. Daoud and J.C. Cousseins, Synth. Metals, **26**, 89 (1988).

21 - T. Mallouk, B.L. Hawkins, M.P. Conrad, K. Zilm, G.E. Maciel and N. Bartlett, Phil. Trans. Roy Soc., London **A314**, 179 (1985).

22 - I. Ohana, Phys. Rev., **B39**, 1914 (1989).

23 - T. Nakajima, M. Molinier and M. Motoyama, Carbon, **29**, 429 (1991).

24 - E.R. Falardeau, L.R. Hanlon and T.R. Thompson, Inorg. Chem., **17**, 301 (1978).

25 - N. Bartlett and B.W. McQuillan in "Intercalation Chemistry", M.S. Whittingham and A.J. Jacobson eds, p.19, Academic Press, New-York (1982).

26 - S. Mouras, A. Hamwi, D. Djurado and J.C. Cousseins, Rev. Chim. Miner., **24**, 572 (1987)

27 - H. Selig in "Inorganic Solid Fluorides", p.354, Academic Press, (1985).

28 - M.S. Dresselhaus and G. Dresselhaus, Adv. Phys., **30**, 139 (1981).

29 - J.E. Fischer in "Intercalated Layered Materials", p. 481, Reidel Publ. (1979).

30 - "Graphite Intercalation Compounds", Part I and Part II, S.A. Solin and H. Zabel eds. Springer Ser. Mater. Sci., Springer, Berlin (1990) and (1992).

31 - R. Hagiwara, M. Lerner and N. Bartlett, J. Chem. Soc. Chem. Commun, p. 573 (1989).

32 - M. Lerner, Ph. D. Thesis, University of California, Berkeley (1988).

33 - H. Takenaka, M. Kawaguchi, M. Lerner and N. Bartlett, J. Chem. Soc. Chem. Commun., p. 1431 (1987).

34 - T. Nakajima, T. Ogawa and N. Watanabe, J. Electrochem. Soc., **134**, 8 (1987). J. Fluorine Chem. **40**, 407 (1988).

35 - J. Kouvetakis, T. Sasaki, C. Shen, R. Hagiwara, M. Lerner, K.M. Krishnam and N. Bartlett, Synth. Metals, **34**, 1 (1989).

36 - H. Touhara, K. Kadono, H. Imoto, N. Watanabe, A. Tressaud and J. Grannec, Synth. Metals, **18**, 549 (1987).

37 - K. Amine, Ph. D. Thesis, University of Bordeaux (1989).

38 - K. Amine, A. Tressaud, H. Imoto, E. Fargin, P. Hagenmuller and H. Touhara, Mat. Res. Bull., **26**, 337 (1991).

39 - A. Tressaud, K. Amine, S.G. Mayorga, E. Fargin, J. Grannec, P. Hagenmuller and T. Nakajima, Eur. J. Solid State Inorg. Chem., **29**, 947 (1992).

40 - H. Touhara, K. Kadono, N. Watanabe and M. Endo, J. Chim. Phys., **81**, 841 (1984).

41 - T. Nakajima, T. Ino, N. Watanabe and H. Takenaka, Carbon, **26**, 397 (1988).

42 - T. Nakajima, N. Watanabe, I. Kameda and M. Endo, Carbon, **24**, 343 (1986).

43 - A. Tressaud, P. Dordor, E. Marquestaut, P. Hagenmuller, H. Fujimoto and S. Flandrois, Synth. Metals, **40**, 179 (1991).

44 - J. Shioya, M. Matsubara and S. Murakami, Synth. Metals, **14**, 113 (1986).

45 - S. Flandrois, B. Hun, J. Grannec, A. Tressaud and C. Hauw, Synth. Metals, **23**, 435 (1988).

46 - C. Cartier and M. Verdaguer, J. Chim. Phys., **86** (7/8) (1989).

47 - K. Amine, A. Tressaud, H. Imoto, J. Grannec, J.M. Dance and C. Hauw, J. Solid State Chem., **96**, 287 (1992).

48 - L. Fournes, T. Roisnel, J. Grannec, A. Tressaud, P. Hagenmuller, H. Imoto and H. Touhara, Mat. Res. Bull., **25**, 79 (1990).

49 - F. Baron, S. Flandrois, C. Hauw and J. Gaultier, Solid State Commun., **42**, 759 (1982).

50 - K. Amine, A. Tressaud, S.G. Mayorga, J. Grannec, P. Hagenmuller, L. Piraux, J.P. Issi and T. Nakajima, J. Fluor. Chem., **57**, 35 (1992).

51 - C. Rigaux in "Proceedings 10th Course Erice Summer School", NATO ASI Series. Series B Physics, p. 235, Plenum Press, New-York (1986).

52 - A. Michalowicz in "Structures fines d'absorption X en Chimie", H. Dexpert, A. Michalowicz and M. Verdaguer eds. CNRS, Paris (1988).

53 - BK Teo,"EXAFS : Basic Principle and Data Analysis", Springer, Berlin (1986).

54 - D.C. Sayers and B.A. Bunker "X-ray absorption", D.C. Kroningsberger and R. Prins eds., Wiley, New-York (1988).

55 - C. Meschi, J.P. Manceau, S. Flandrois, P. Delhaes, A. Ansaert and L. Deschamps, Ann. Phys., **11**, 199 (1986).